

Role of Amines in the Mitigation of CO₂ Top of the Line Corrosion

Z. Belarbi,^{‡*} F. Farelas,^{*} M. Singer,^{*} and S. Nešić^{*}

ABSTRACT

The principal objective of this work is to investigate and understand the top of the line corrosion (TLC) inhibition mechanism in the presence of amines: diethylamine and morpholine. TLC can be defined as corrosion of carbon steel under water condensation conditions in the presence of acid gases such as CO₂, which can be a problem in wet natural gas transportation lines. In order to define the possible interactions between the tested amines and the steel surface, the surface charge was investigated by determining the potential of zero charge (PZC). The PZC was measured by means of electrochemical impedance spectroscopy (EIS) in a 1 wt% NaCl solution at different pH values. The possible inhibitive properties of diethylamine and morpholine were first tested under full immersion in the water phase—a condition corresponding to the so-called “bottom of the line” situation in gas pipelines, using linear polarization resistance and EIS. This was followed by tests in the gas phase under water condensing conditions, corresponding to TLC, when the weight loss method was used to measure the corrosion rate. After the experiments, the steel surface was characterized by scanning electronic microscopy. The inhibition was affected by the surface charge that provided key information about the mechanism of adsorption of amines (diethylamine and morpholine) on the steel surface. In addition, the effect of inhibition of corrosion rate was directly linked to the change in solution pH. Considering that the amines were almost fully protonated in the range of pH tested here, their vapor pressures and consequently their

concentration in the condensed water was very low. Given that there was no chloride in the condensed water, this further limited the inhibitive effect. In addition, when adsorbed at the surface, diethylamine and morpholine did not seem to demonstrate any significant filming properties because of the weak interaction of the nonpolar groups in the amine molecules.

KEY WORDS: bottom of the line corrosion, CO₂ corrosion, inhibition, morpholine, potential of zero charge, top of the line corrosion, volatile amine

INTRODUCTION

Top of the line corrosion (TLC) is a phenomenon encountered in wet natural gas transportation, when problems of corrosion appear inside the pipe as a result of the condensation of water vapor containing dissolved acid gases, such as CO₂. One way to minimize TLC of carbon steel pipelines exposed to CO₂ environments is by the use of volatile corrosion inhibitors (VCIs). VCIs used in industry are often a complex mixture of several compounds, e.g., imidazolines salts and light amines (triethylenetetramine, diethylamine, methoxypropylamine, and pyridine salts) in particular ratios.¹⁻³

A large variety of VCIs (mixture of amines and carboxylic acids) have been used successfully for the protection of metallic equipment against atmospheric corrosion during storage and transportation.⁴⁻⁶ Cyclohexylamine carbonate has been found to be an effective VCI for Nd-Fe-B alloys in simulated atmospheric environments, as well as under thin electrolyte layers.⁷ Morpholine has been used as a corrosion

Submitted for publication: April 21, 2016. Revised and accepted: June 25, 2016. Preprint available online: June 27, 2016, <http://dx.doi.org/10.5006/2121>.

[‡] Corresponding author. E-mail: belarbi@ohio.edu.

^{*} Institute for Corrosion and Multiphase Technology, Department of Chemical and Biomolecular Engineering, Ohio University, Athens, OH 45701.

inhibitor and VCI for carbon steel exposed to alkaline conditions⁸ and 2N H₂SO₄ and 2N H₃PO₄ solutions.⁹ It has been shown that a better inhibition was obtained in 2N phosphoric acid because in H₃PO₄ solution phosphate ions probably form a bridge between the protonated molecules of inhibitors and facilitate the adsorption of inhibitor molecules, while in H₂SO₄ this bridge is not formed as a result of low charge of sulfate ions. Morpholine and its derivatives have been used to prevent the corrosion of metal surfaces during transport and storage of equipment.¹⁰ Morpholinium oligomer (MPO) has also shown to be a good vapor corrosion inhibitor for steels exposed to atmospheric conditions. The MPO has a larger molecular size than morpholine; thus, it has larger coverage on the metal surface, providing better inhibition.¹¹ Diethylamine was tested in petroleum/water corrosive mixtures at 25°C¹² and has been used as corrosion inhibitor for carbon steel in aqueous solution at pH of 11.4. The results showed that the presence of diethylamine induced the formation of a layer providing protective properties to the metal.¹³

In order to understand how amines interact with the steel surface, it is important to analyze the fundamentals of inhibitor adsorption. The level of adsorption of amines depends on their chemical structure, aqueous environment (acid or basic solution), metal surface condition, and electrochemical potential at the interface. The adsorption process is governed by the so-called “charge” on the metal surface and the chemical structure of the inhibitor. Physical adsorption is a result of the electrostatic attraction between the inhibiting ions and the electrochemically charged surface of the metal, which is defined by the position of the open-circuit corrosion potential (OCP) with respect to the potential of zero charge (PZC). PZC is the potential of the where both the solution side and the metallic side of the interface have a zero net charge, offering itself as a natural potential reference point used to identify any other net surface charge. If the metal potential is higher than the potential of zero charge, the metal is said to be positively charged with respect to the PZC and the adsorption of anions from the solution is favored. Conversely, the adsorption of cations is preferred if the free corrosion potential is lower than PZC.¹⁴⁻¹⁵

The objective of this paper is to investigate and understand the TLC inhibition mechanism in the presence of diethylamine and morpholine by identifying the type of bond between amines and the carbon steel surface. In order to understand the role of amines in CO₂ corrosion, carbon steel samples were first immersed in a 1 wt% sodium chloride (NaCl) solution in order to enable electrochemical measurements. This situation corresponds to the so-called bottom of the line corrosion (BLC) in wet gas lines, where

there is a continuous water layer present. The corrosion behavior of carbon steel with and without amines was evaluated using linear polarization resistance (LPR) and electrochemical impedance spectroscopy (EIS) measurements.

For TLC experiments, weight loss (WL) carbon steel samples were used and flush mounted at the top of the experimental setup. This enabled comparison and validation of inhibition mechanism for the two scenarios: under constant water immersion and under condensing water conditions. In addition, the pH was measured both for the bulk solution and for condensed water, before and after adding amines, in order to properly identify the role of amines in corrosion inhibition.

While the performance of these amines under BLC conditions was previously evaluated, no results have been reported in the literature on the performance of diethylamine and morpholine as VCI for CO₂ corrosion at the top of the line, where they have been often used in commercial applications.

EXPERIMENTAL PROCEDURES

Materials and Chemicals

The analytical grade amines (morpholine and diethylamine) used in this research were acquired from Sigma-Aldrich[†]. Steel samples used for electrochemical and weight loss measurements were made of API 5L X65 carbon steel with a tempered martensite microstructure. NaCl was dissolved in deionized water that was saturated with CO₂. The chemical composition of the carbon steel is provided in Table 1.

Electrochemical Measurements (Bottom of the Line Corrosion)

For BLC experiments, an electrochemical cell with a three-electrode configuration was used (Figure 1). A carbon steel API X65 rotating cylinder electrode (RCE), a platinum grid, and an Ag/AgCl_{sat} electrode were used as working, counter, and reference electrodes, respectively. The reference electrode was placed in a separate chamber and was connected to the corrosion cell via a KCl salt bridge and a Luggin capillary. The RCE was ground with silicon carbide paper (600 grit), cleaned with isopropanol in an ultrasonic bath, and air-dried before introduction into the cell. All of the experiments were performed in deionized water containing 1 wt% NaCl at 25°C. The solution was deoxygenated for 2 h by sparging with CO₂ prior to the

TABLE 1
Composition (wt%) of API 5L X65 Carbon Steel

| Element | C | Nb | Mn | P | S | Ti | V | Ni | Fe |
|---------|------|------|------|-------|--------|------|------|------|---------|
| X65 | 0.05 | 0.03 | 1.51 | 0.004 | <0.001 | 0.01 | 0.04 | 0.04 | balance |

[†] Trade name.

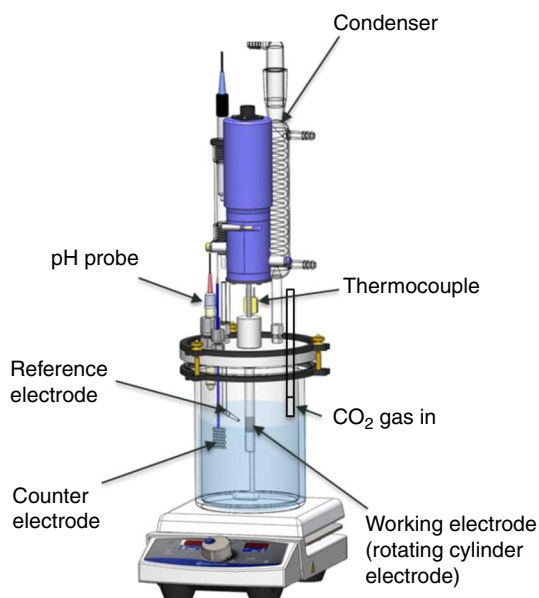


FIGURE 1. Experimental setup for electrochemical experiments (BLC).

TABLE 2

Experimental Matrix for Identification of Steel Surface Charge

| | |
|------------------------|------------------|
| Total pressure (bar) | 1 |
| pCO ₂ (bar) | 0.96 |
| Solution | 1 wt% |
| pH | 3.8, 5.1, 5.3 |
| Solution temperature | 25°C |
| Working electrode | X65 carbon steel |
| Speed (rpm) | 1,000 |

introduction of the working electrode. To avoid possible noise in electrochemical measurements caused by CO₂ sparging, the sparge tube was pulled up into the headspace during the measurements while the CO₂ was purged continuously in order to avoid oxygen contamination and to maintain saturation of the test solution with CO₂. A pH probe was used to measure the pH of the solution before and after adding the amine. The rotation speed of the working RCE was set at 1,000 rpm before starting any electrochemical measurement.

The PZC was identified by means of EIS at different pH. Prior to any measurement, the OCP was monitored for about 8 min to 10 min to ensure a stable value, which was typically within 5 mV of the initial value, and the fluctuation of the OCP was $< \pm 1$ mV. EIS was conducted at different potentials with respect to the OCP using the frequency range of 10 kHz to 0.1 Hz, by taking seven points per decade. The amplitude was 10 mV (root mean square) from the applied potential. The experimental matrix is shown in Table 2.

TABLE 3

Experimental Matrix for Bottom of the Line Corrosion (BLC)

| | |
|----------------------------|------------------|
| Total pressure (bar) | 1 |
| pCO ₂ (bar) | 0.96 |
| Solution | 1 wt% |
| Solution temperature | 25°C |
| Working electrode | X65 carbon steel |
| Amines (ppm _v) | 0, 100, 400, 800 |
| Speed (rpm) | 1,000 |

Corrosion rate was assessed by LPR, by polarizing the working RCE by ± 5 mV from the OCP, using the scan rate of 0.125 mV/s and B value of 26 mV. LPR and EIS measurements were taken every 40 min during the total exposure time of 14 h. All measurements were performed using a Gamry[†] potentiostat/galvanostat. The full experimental matrix for BLC experiments is shown in Table 3.

Weight Loss Measurements (Top of the Line Corrosion)

The experimental setup used for evaluating the efficacy of VCIs under TLC conditions is shown in Figure 2. As the conductivity of condensed water is very low and the condensed water layer is not stable over time, may be discontinuous, and is often very thin, it is difficult to perform electrochemical measurements on samples exposed to TLC conditions, so the WL technique was used to measure the time-averaged corrosion rate at the top of the line. A WL carbon steel API X65 specimen in the form of a disc (exposed area = 7.92 cm²) was prepared following the same procedure described in the previous section. The WL specimen was flush-mounted at the top of the experimental setup, and its

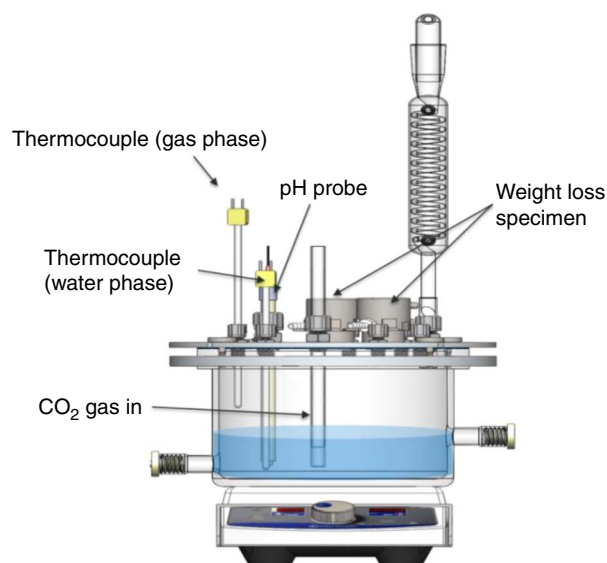


FIGURE 2. Experimental setup for evaluating efficacy of VCI candidates for TLC.

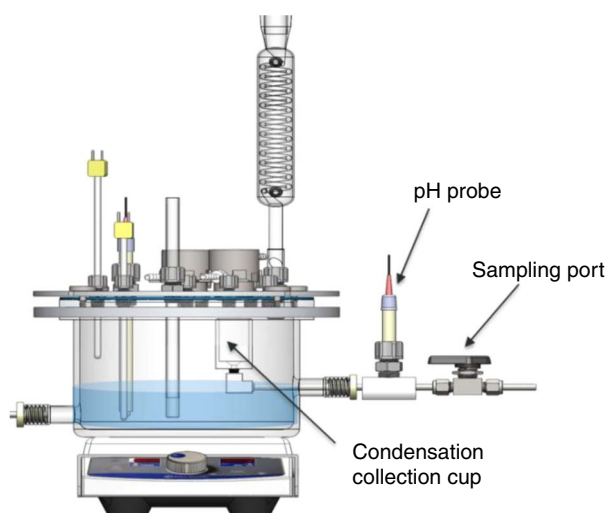


FIGURE 3. Experimental setup for measuring the pH of the condensed water under TLC conditions.

temperature was controlled at 32°C using a cooling coil. In order to have condensation, the gas temperature was set to 65°C, while the aqueous solution at the bottom of the cell was maintained at 72°C.

Weight loss corrosion rate was determined by following the ASTM Standard G1,¹⁶ as follows:

$$CR = (K \times W) / (A \times t \times \rho) \quad (1)$$

where CR: corrosion rate in mm/y, K: conversion factor $8.76 \times 10^4 = 24 \text{ h/d} \times 365 \text{ d/y} \times 10 \text{ mm/cm}$, W: weight loss in g, A: area in cm^2 , t: time of exposure in h, and ρ : density of steel, 7.87 g/cm^3 .

A pH probe was used to measure the pH in the bottom solution before and after adding the VCI. The experimental setup used for measuring the pH of the condensed water under TLC conditions is shown in Figure 3. In order to distinguish the effect of amine on the pH of condensed water from the effect caused by dissolved iron ions, a Type 304 (UNS S30400⁽¹⁾) stainless steel specimen (exposed area = 7.92 cm^2) was used and prepared following the same procedure as described in the previous section. The condensed water was collected in the condensation collection cup and the pH was measured in situ as shown in Figure 3. The detailed TLC experimental matrix for the experimental work is shown in Table 4.

Surface analysis of the exposed electrode was investigated by scanning electron microscopy (SEM). Imaging was performed at an accelerating voltage of 15 kV using a secondary electron signal.

⁽¹⁾ UNS numbers are listed in *Metals and Alloys in the Unified Numbering System*, published by the Society of Automotive Engineers (SAE International) and cosponsored by ASTM International.

TABLE 4

Experimental Matrix for Top of the Line Corrosion (TLC)

| | |
|--|------------------|
| Total pressure (bar) | 1 |
| pCO ₂ (bar) | 0.66 |
| Solution | 1 wt% |
| Solution temperature at the bottom | 74±2°C |
| Gas temperature | 65±2°C |
| Sample temperature | 32±2°C |
| Water condensation rate (mL/m ² /s) | 0.6 |
| Working electrode | X65 carbon steel |
| Amines (ppm _v) | 0, 400 |

RESULTS AND DISCUSSION

Identification of Steel Surface Charge

The phenomenon of adsorption is influenced by the chemical structure of the inhibitor, the charge distribution or dipole moment of the inhibitor molecules, and the charge of the metal surface. The metal surface charge is defined by the position of the free corrosion potential (OCP) with respect to its PZC. The PZC is extremely sensitive to surface conditions (e.g., pH, impurities), with pH being the most important factor.¹⁷⁻¹⁸ Taking into account the previous statement, experiments were performed at pH values of 3.8, 5.1, and 5.3. The pH 3.8 was the “natural” value obtained when water was saturated with 1 bar (100 kPa) CO₂ at room temperature (25°C), while pH values of 5.1 and 5.3 were obtained after adding 400 ppm_v of diethylamine or morpholine, respectively. In order to determine if the change of the PZC after addition of the amines was solely a result of a change of pH, an experiment at pH 5.3 without inhibitor was performed first to have a reference point. It is important to mention that these pH values fall within the typical range found in condensed water.

According to Lorenz, et al.,¹⁹ the PZC can be determined from EIS measurements through the calculation of the double layer capacitance, C_{dl} . In this research project, to identify the C_{dl} , EIS measurements were recorded at different potentials with respect to the OCP on a freshly polished electrode (see Figure 4).

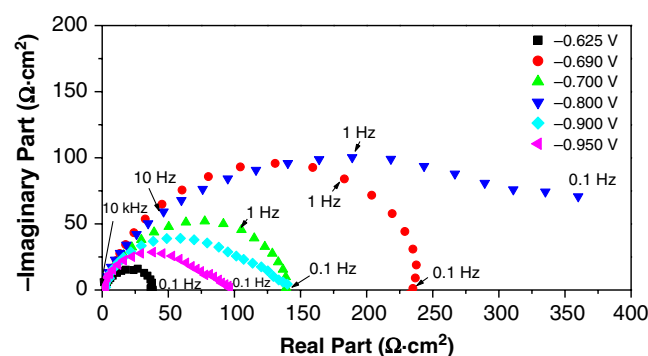


FIGURE 4. Nyquist plot of carbon steel in 1 wt% NaCl solution at 25°C as a function of potential. pH = 5.3.

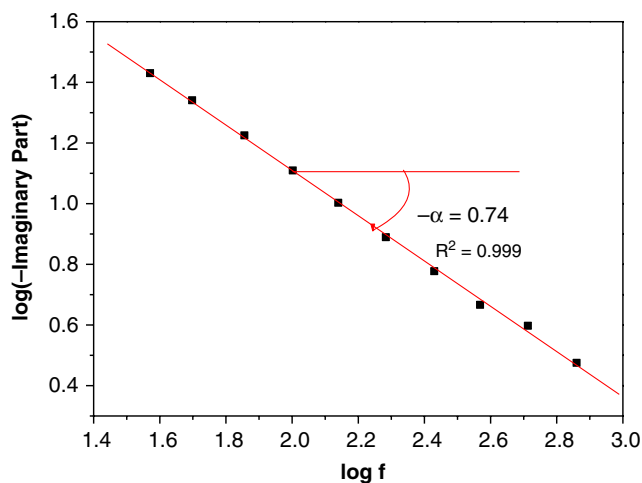


FIGURE 5. Representation of the logarithm of the imaginary part of the impedance vs. the logarithm of the frequency at the potential of $-0.7 V_{Ag/AgCl}$ and pH 5.3. The slope of the red line leads to the α coefficient in Equation (2) being obtained.

There, it can be seen that for pH 5.3 there is a depressed charge-transfer semicircle which is characteristic of non-uniform metal surface. In that situation the capacitance, C_{dl} , is replaced in the analysis by a so-called “constant phase element” (CPE).²⁰ The same behavior was seen at pH 5.1 and 3.8 (not shown in this manuscript).

To confirm the existence of the CPE, the logarithm of the imaginary part of the impedance was plotted with respect to the logarithm of the frequency in the high-frequency domain (Figure 5). The impedance of the CPE is defined as follows:²⁰

$$Z_{CPE} = \frac{1}{Q_{eff}(j\omega)^\alpha} \quad (2)$$

where $0 < \alpha < 1$ and Q_{eff} is the CPE coefficient, which can be interpreted as the effective high-frequency capacitance. The value of the slope of the continuous line, shown in Figure 5, provides the coefficient $\alpha = 0.74$ at $-0.7 V_{Ag/AgCl}$ and pH 5.3, which confirms the presence of the CPE in the high-frequency domain. The Q_{eff} can be obtained directly from the imaginary part of the impedance as:

$$Q_{eff} = -\sin\left(\frac{\alpha\pi}{2}\right) \frac{1}{(2\pi f)^\alpha \text{Im Part}} \quad (3)$$

The calculated Q_{eff} vs. frequency is plotted in Figure 6. The asymptotic value of Q_{eff} obtained at high frequency is the best estimate of the double layer CPE coefficient and is termed Q_{dl} .²⁰ It is important to point out that the assessment of Q_{dl} should be made at frequencies significantly larger than the largest characteristic relaxation frequency for the system. Only in this range, the error in assessment of Q_{dl} is of the

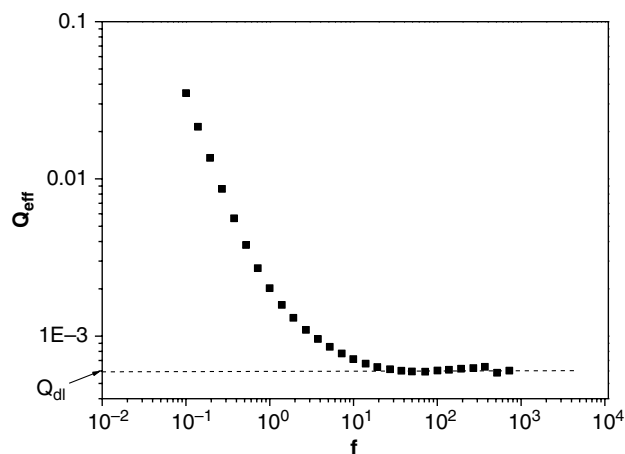


FIGURE 6. Effective CPE coefficient defined by Equation (3) as a function of frequency at $-0.7 V_{Ag/AgCl}$ and pH 5.3.

order of 1%. Note that for a value of $\alpha = 1$, the Q_{dl} value directly corresponds to C_{dl} . This was the first step toward interpretation and evaluation of impedance data, and does not depend on any specific equivalent circuit model.

Finally, the equation proposed by Brug, et al.,²¹ is used to calculate the value of C_{dl} given that the values of Q_{dl} , α , and solution resistance R_s are known:

$$C_{dl} = R_s^{\frac{1-\alpha}{\alpha}} Q_{dl}^{\frac{1}{\alpha}} \quad (4)$$

The solution resistance (R_s) is found at the intersection of the high-frequency impedance with real axis in the Nyquist plot (Figure 4).

Figure 7 represents the C_{dl} values calculated from Equation (4) with respect to the applied potential, E , at different pH. The minimum value on the C_{dl} vs. E curve represents the PZC of the electrode. The PZC is the point where the double layer changes its polarity. The values of PZC at the selected pH values are shown in Table 5. As it can be seen, the values of PZC obtained at pH 5.1 and 5.3 are more negative than those observed at pH 3.8. Such an effect may be a result of the change of the species concentration in solutions (in this case H^+ ions in an acidic solution).²² Comparing the values of the PZC with the corresponding OCP values, it is possible to deduce that the steel surface is positively charged with respect to the PZC at the conditions of the present study (see Table 5).

Figures 8 and 9 show the likely mechanism of electrostatic adsorption of amines on a positively charged steel surface exposed to NaCl solutions.^{14,23} In solutions with dissolved CO_2 (mildly acidic solutions), amines quickly protonate as a result of their basicity. The Cl^- ions and water molecules adsorb on the steel surface and interact with the

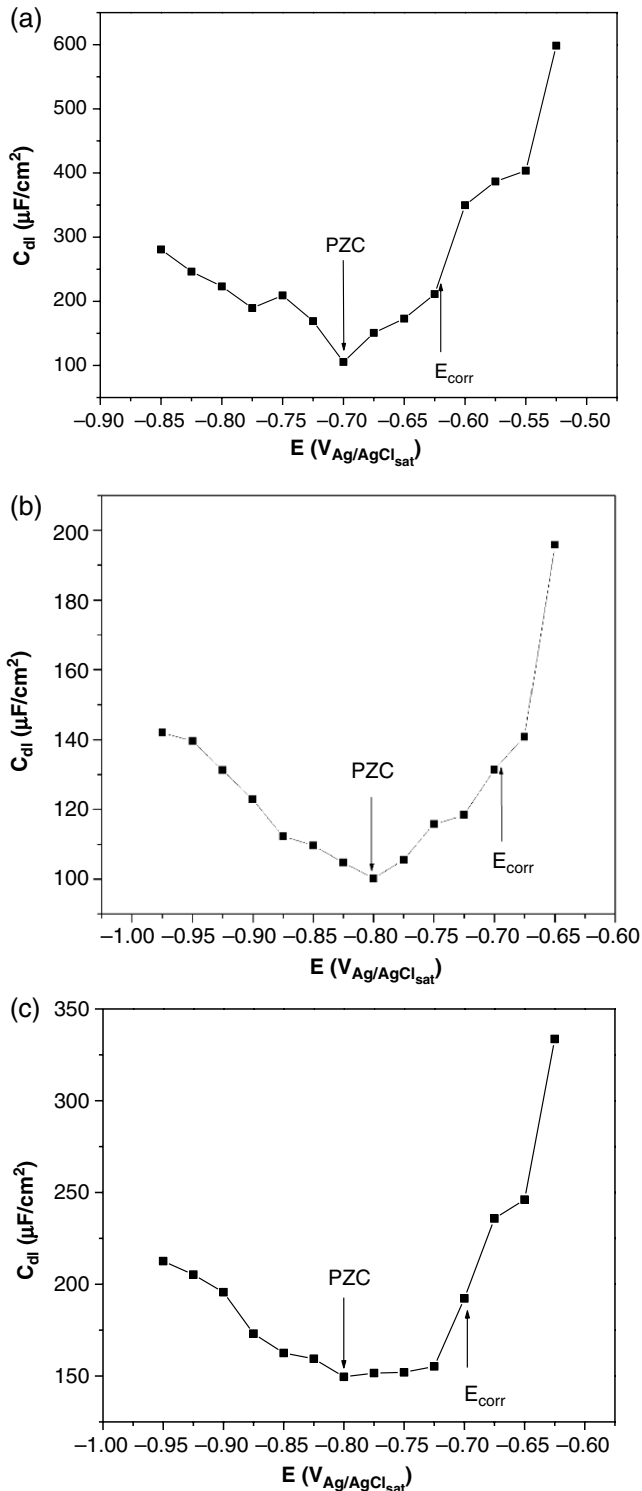


FIGURE 7. C_{dl} value calculated from Equation (5) with respect to applied potential at different pH. (a) pH=3.8, (b) pH=5.1, and (c) pH=5.3.

protonated amine forming electrostatic bonds (Figure 8). Protonated amine molecules can adsorb on the steel surface only if they are charged negatively; otherwise, they need intermediates such as Cl^- ions.

TABLE 5

Values of the PZC and (OCP-PZC) Recorded for Carbon Steel Electrode Immersed in 1 wt% NaCl Solutions in the pH Range (3.8 to 5.3) at 25°C

| | pH 3.8 | pH 5.1 | pH 5.3 |
|------------------------------|--------|--------|--------|
| PZC ($V_{\text{Ag/AgCl}}$) | -0.7 | -0.8 | -0.8 |
| OCP ($V_{\text{Ag/AgCl}}$) | -0.62 | -0.68 | -0.69 |
| OCP-PZC (V) | 0.08 | 0.12 | 0.11 |

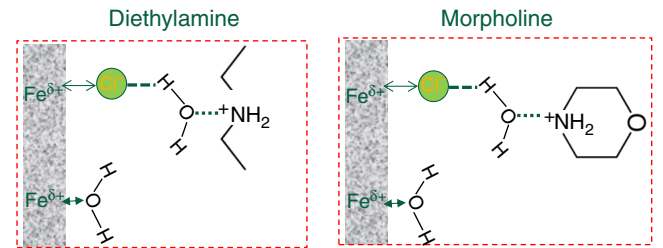


FIGURE 8. Possible interactions between protonated amine functional groups and metal surface.^{14,23} (\leftrightarrow): Electrostatic interaction between induced dipole ($\text{Fe}^{\delta+}$) and anion (Cl^-). (-): Hydrogen bonding. (\dots): Electrostatic interaction between permanent dipole (H_2O) and cation ($-\text{NH}_3^+$). ($\leftarrow\rightarrow$): Van der Waals bonding.

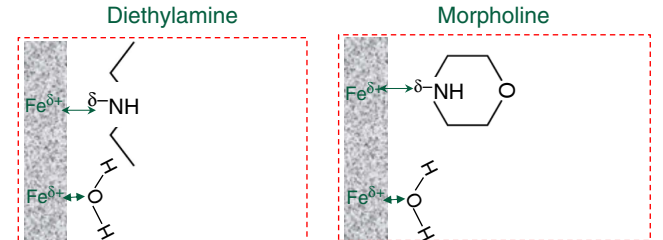


FIGURE 9. Possible interactions between nonprotonated amine functional groups and metal surface.^{14,23} (\leftrightarrow): Van der Waals bonding.

For the case of unprotonated amines, the nitrogen atom (heteroatom) has a free electron pair that can form Van der Waals bonding with the steel surface; see a possible configuration in Figure 9. In both cases (protonated and unprotonated), amines can easily desorb because they do not form a strong (chemical) bond. The formation of a donor-acceptor bond between the metal and inhibitor is not possible because the non-oxidized steel surface is not an electron acceptor. In order to form a donor-acceptor bond, the acceptor should have an opening in the outer electron orbitals, available to accept two electrons. In addition, the oxygen atom of the morpholine molecule cannot form Van der Waals bonding with the steel surface because it has an even lower

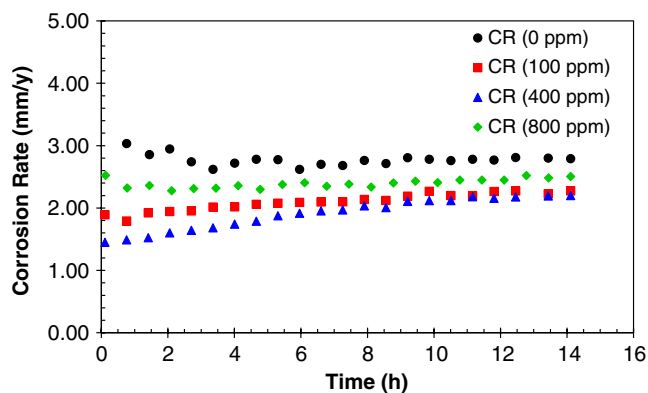


FIGURE 10. BLC rate of carbon steel RCE immersed in 1 wt% NaCl solution in presence and absence of morpholine at 25°C as a function of time.

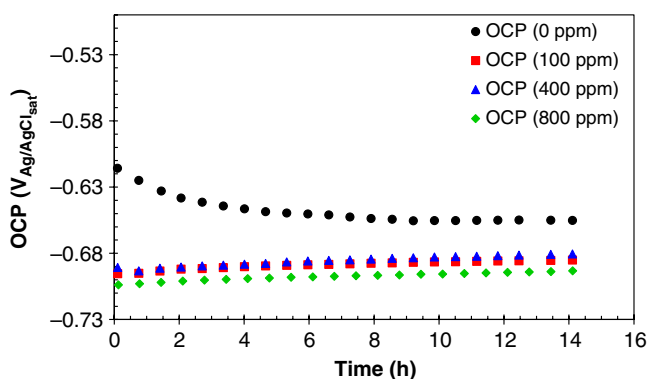


FIGURE 11. OCP of carbon steel RCE immersed in 1 wt% NaCl solution in presence and absence of morpholine at 25°C as a function of time.

electron-donor capability than nitrogen atom in the same molecule.²⁴

Bottom of the Line Corrosion Experiments

In order to study the inhibition by the selected amines, the experiments were performed first with the specimen fully immersed in the water phase followed by experiments in the gas phase. The results for morpholine are shown in Figures 10 and 11. In the absence of amine, corrosion rate (CR) was 2.8 mm/y and OCP was $-0.64 V_{Ag/AgCl}$. In the presence of morpholine, the final CR did not significantly change with concentration (around 2 mm/y). When compared to the uninhibited condition (2.8 mm/y), the decrease was not practically significant. The OCP after adding amines became more negative. Such an effect is most likely a result of the decrease in H^+ ion reduction at the steel surface (from increase of pH).

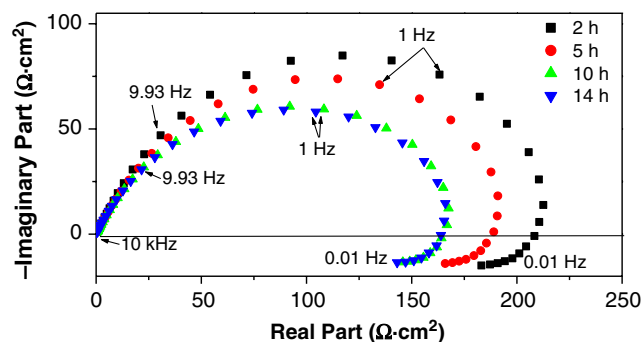


FIGURE 12. The Nyquist plot of carbon steel immersed in 1 wt% NaCl solution at 25°C as a function of time in the presence of 400 ppm_v morpholine.

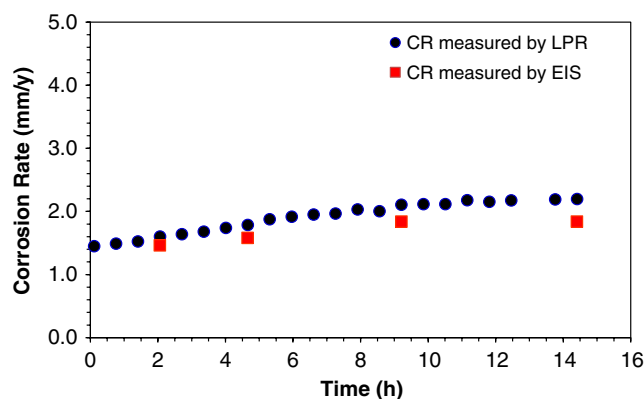


FIGURE 13. Comparison between CR measured by LPR and CR measured by EIS in the presence of 400 ppm_v morpholine.

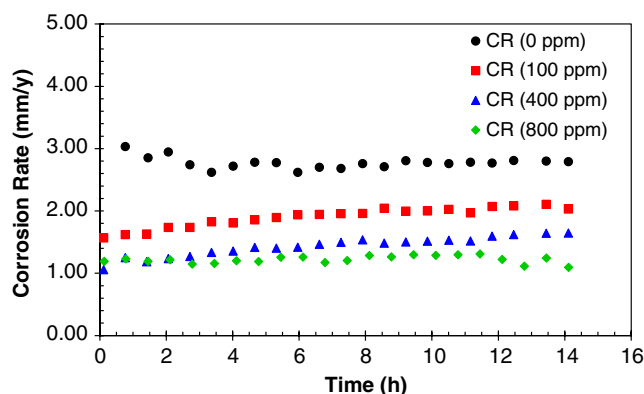


FIGURE 14. BLC rate of carbon steel RCE immersed in 1 wt% NaCl solution in presence and absence of diethylamine at 25°C as a function of time.

Figure 12 shows the impedance diagrams in the Nyquist plane at different times. One can see depressed semicircles at high to medium frequencies and inductive loops at low frequencies. The

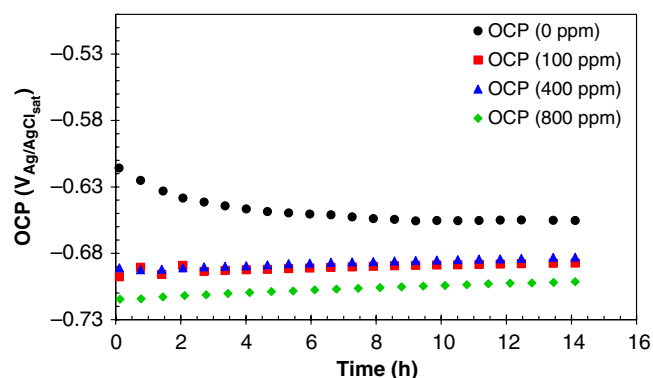


FIGURE 15. OCP of carbon steel RCE immersed in 1 wt% NaCl solution in presence and absence of diethylamine at 25°C as a function of time.

TABLE 6

Comparison of the Measured Corrosion Rate and Calculated Corrosion Rate Resulting from a pH Change

| Chemicals | Measured pH | Measured CR (mm/y) | Calculated CR Using Software (mm/y) | Measured CR Without Adding Amine at the Same pH (mm/y) |
|--------------------------------------|-------------|--------------------|-------------------------------------|--|
| Blank | 3.8 | 2.8 | 4.6 | — |
| Morpholine (400 ppm _v) | 5.3 | 1.9 | 1.6 | 1.85 |
| Diethylamine (400 ppm _v) | 5.1 | 1.4 | 1.6 | — |

high-frequency semicircles are associated with the time constant of the charge transfer process and the double layer capacitance. The inductive loop may be attributed to the relaxation process obtained by adsorbed species such as Cl_{ads}^- and H_{ads}^+ on the electrode surface. The presence of morpholine increases the impedance but does not change other aspects of the process. The charge transfer resistance, R_t , is given by the intersection of the low-frequency end of the Nyquist curves with the abscissa. The R_t was used as an alternative method to calculate the CR. Figure 13 shows a good agreement between CR measured by LPR and EIS. The same behavior is observed in the presence of diethylamine (Figures 14 and 15).

In the light of these measurements, one can conclude that morpholine and diethylamine have shown poor inhibition of carbon steel immersed in a mildly acidic CO_2 -containing environment. In order to clarify if the decrease of corrosion rate after the

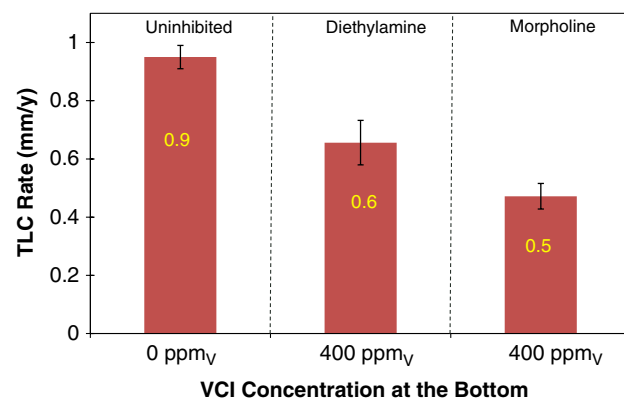


FIGURE 16. Corrosion rate by weight loss measurement of the TLC specimens (water condensation rate = 0.6 mL/m²/s) with and without amines. Note: VCI candidate concentrations on x-axis are the injected concentration for the bottom solution.

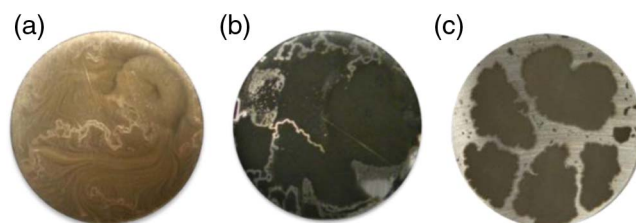


FIGURE 17. Visual images of sample exposed to corrosion in the co-condensation of water (water condensation rate = 0.6 mL/m²/s) in the presence of (a) no inhibitor, (b) 400 ppm_v diethylamine, and (c) 400 ppm_v morpholine after 2 d.

addition of the amines was a result of the increase of pH or a result of the adsorption of amines on the steel surface, a comparison between the measured corrosion rate and calculated corrosion rate using MULTICORP^{†,(2)} was performed, shown in Table 6. The corrosion rates after the addition of the amines (at 400 ppm_v) are similar to the calculated corrosion rate in the absence of the amines but at the same pH. Therefore, the decrease of corrosion rate could be ascribed to the increase of pH and not to the adsorption of the neutral amines. It is understandable because these amines were easily protonated in the acid solution, the ratio of $[\text{Amine}]/[\text{AmineH}^+]$ being equal to $10^{-8.5}$ and 10^{-11} for morpholine and diethylamine, respectively.

Top of the Line Corrosion Experiments

The comparison of TLC rates obtained by WL is shown in Figure 16, followed by surface images taken after the tests, shown in Figure 17. The error bars in Figure 16 represent the standard deviation between two weight loss samples. The results show that without the inhibitor present, the carbon steel specimen was

⁽²⁾ Software developed by Institute for Corrosion and Multiphase Technology, Ohio University.

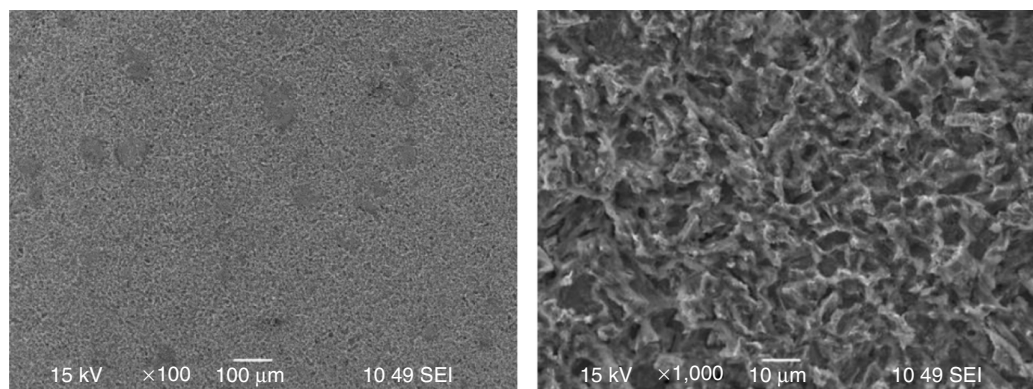


FIGURE 18. SEM images at different magnifications of the blank sample after 2 d.

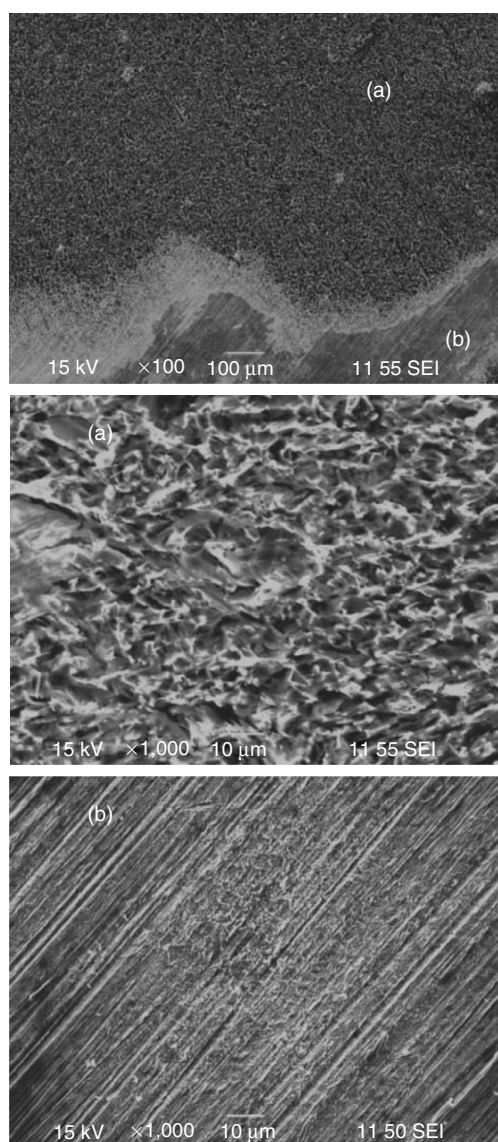


FIGURE 19. SEM images at different magnifications and locations ([a] corroded surface and [b] protected surface) of the sample in the presence of 400 ppm of morpholine after 2 d.

corroding at a time averaged (TLC) rate of 0.9 mm/y, and its surface was fully covered by a corrosion product layer. In the presence of diethylamine and morpholine, the corrosion rate at the top decreased to 0.6 mm/y and 0.5 mm/y, respectively. As most of the morpholine and diethylamine were protonated in the solution at the bottom of the cell, the concentration in solution should be almost constant because the protonated inhibitor cannot evaporate. In order to avoid any losses of the nonprotonated inhibitor in the gas phase, a condenser was used. It can be hypothesized that when the evaporated amine dissolved in the condensed water at the top, it increased the pH, thereby decreasing the TLC rate. In order to corroborate this hypothesis, the condensed water was collected in the condensation collection cup and the pH was measured in situ over 2 d. The average pH of the condensed water increased from pH 4.3 in the absence of inhibitor to pH 4.7 and 4.8 after adding morpholine and diethylamine, respectively. It was explained in the previous section that amines do not form an adsorbed layer as a result of the positively charged steel surface in the absence of chlorides. The same behavior should be expected at the top of the line, and as in the condensed water there are no chloride ions, so no adsorption of protonated amine on the steel surface was expected.

The results show that morpholine and diethylamine did not fully protect the steel specimen exposed to the TLC conditions. The SEM images of this specimen surface (Figures 18 through 20) confirmed this conclusion, showing alternating corroded and protected areas, especially in presence of morpholine. The protonated morpholine molecule contains an oxygen atom that could form an electrostatic bond with the positively charged surface. In this case, the oxygen atom displays electron-donor capability, while the nitrogen atom does not, as it is protonated. This can lead to adsorption of protonated morpholine on the steel surface, via the oxygen. However, the reason why this adsorption has not been uniform, leaving the steel surface only partially protected,

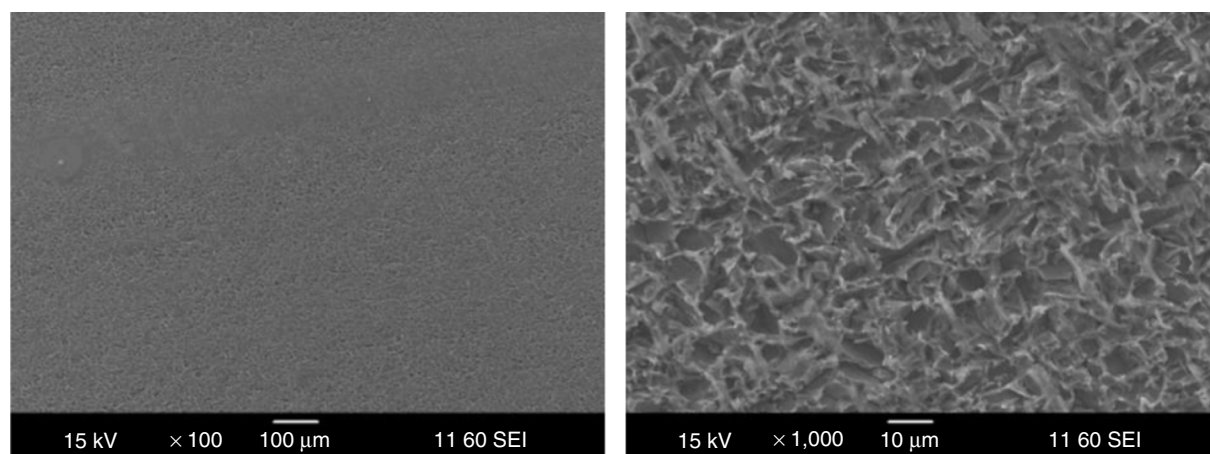


FIGURE 20. SEM images at different magnifications of the sample surfaces in the presence of 400 ppm of diethylamine after 2 d.

remains unclear. More experiments, possibly considering the use of force spectroscopy, need to be done in order to explain this phenomenon. Literature indicates that in alkaline environments, these amines have been successfully used because they exist as neutral molecules and the metal surface is probably changed (resulting from the presence of oxides).⁸

CONCLUSIONS

In this work, electrochemical techniques of electrochemical impedance spectroscopy, linear polarization resistance, and the weight loss method were used to study bottom of line corrosion to help with the understanding of top of the line inhibition mechanism in the presence of diethylamine and morpholine in a CO₂ environment and mildly acidic pH. The mechanisms were investigated by studying the inhibitor interaction with the steel surface. As a result of this study, the following conclusions were drawn:

- ❖ The corroding steel surface is positively charged with respect to the potential of zero charge (PZC); therefore, the adsorption of anions (Cl⁻) or permanent dipole is favored at the bottom of the line.
- ❖ The type of bonding and related interaction between amines and steel surface were identified by considering the steel surface charge: it was found that the type of bonding is governed by electrostatic interactions.
- ❖ A rather small decrease of TLC rate in the presence of morpholine and diethylamine could be attributed to the increase of pH after their addition into the aqueous solution.
- ❖ Morpholine and diethylamine were protonated in acidic solutions and did not have significant filming properties.

ACKNOWLEDGMENTS

The author would like to thank the following companies for their financial support: Apache, BHP Billiton, BP, Chevron, ConocoPhillips, MI-SWACO, PETRONAS, PTTEP, Woodside, and Talisman.

REFERENCES

1. R.L. Martin, "Inhibition of Vapor Phase Corrosion in Gas Pipelines," CORROSION 1997, paper no. 337 (Houston, TX: NACE International, 1997).
2. R.L. Martin, *Corrosion* 49, 8 (1993): p. 694.
3. R.L. Martin, "Control of Top-of-Line Corrosion in a Sour Gas Gathering Pipeline with Corrosion Inhibitors," CORROSION 2009, paper no. 288 (Houston, TX: NACE, 2009).
4. U. Rammelt, S. Koehler, G. Reinhard, *Corrosion* 67, 4 (2011): p. 045001-1.
5. E. Cano, D.M. Bastidas, J. Simancas, J.M. Bastidas, *Corrosion* 61, 5 (2005): p. 473.
6. A. Wachter, T. Skei, N. Stillman, *Corrosion* 7, 9 (1951): p. 284.
7. X. Zhang, Y. Ma, Y. Li, M.K. Lei, F.H. Wang, *Corrosion* 69, 7 (2013): p. 647.
8. S. Nasrazadani, J. Diaz, J. Stevens, R. Theimer, *Corros. Sci.* 49, 7 (2007): p. 3024.
9. K. Jayanthi, M. Sivaraju, K. Kannan, *E-J. Chem.* 9, 4 (2012): p. 2213.
10. Sudheer, M. Quraishi, E.E. Ebenso, M. Natesan, *Int. J. Electrochem. Sci.* 7 (2012): p. 7463.
11. D.Q. Zhang, L.X. Gao, G.D. Zhou, *Corrosion* 61, 4 (2005): p. 393.
12. H.A. Sorkhabi, S.A.N. Amri, *Acta Chim. Slovenica* 47 (2000): p. 507.
13. V.G. Arriaga, J.A. Ramirez, M. Amaya, E. Sosa, *Corros. Sci.* 52 (2010): p. 2268.
14. E. McCafferty, *Introduction to Corrosion Science* (New York, NY: Springer, 2010), p. 38.
15. M. Yadav, L. Gope, T.K. Sarkar, *Res. Chem. Intermed.* 42, 3 (2016): p. 2641.
16. ASTM G1-90, "Standard Practice for Preparing Cleaning and Evaluating Corrosion Test Specimens" (West Conshohocken, PA: ASTM International, 1999), p. 15.
17. M. Chelveyohan, C.H.B. Mee, *J. Phys. C: Solid State Phys.* 15 (1982): p. 2305.
18. P. Ramirez, R. Andreul, A. Cuestal, C.J. Calzado, J. Calvente, *Anal. Chem.* 79 (2007): p. 6473.
19. W.J. Lorenz, H. Fischer, *Electrochim. Acta* 11 (1966): p. 1597.
20. M.E. Orazem, B. Tribollet, *Electrochemical Impedance Spectroscopy* (Hoboken, NJ: John Wiley & Sons, 2008), p. 333.

21. G.J. Brug, A.G.V.D. Eeden, M.S. Rehbach, J.H. Sluyters, *J. Electroanal. Chem.* 176 (1984): p. 275.
22. M.A. Amin, S.S.A. El-Rehim, E.E.F. El-Sherbini, R.S. Bayoumi, *Electrochim. Acta* 52 (2007): p. 3588.
23. R. Sokoll, H. Hobert, I. Schmuck, *J. Catal.* 121 (1990): p.153.
24. A. Subramanian, M. Natesan, V. Muralidharan, K. Balakrishnan, T. Vasudevan, *Corrosion* 56, 2 (2000): p. 144.